Clinical Science (2014) **126**, 721–726 (Printed in Great Britain) doi: 10.1042/CS20130326

Original Paper

Detection of mutations in *KLHL3* and *CUL3* in families with FHHt (familial hyperkalaemic hypertension or Gordon's syndrome)

Mark GLOVER*, James S. WARE†‡, Amanda HENRY*, Martin WOLLEY§, Roddy WALSH†, Louise V. WAIN¶, Shengxin XU§, William G. VAN'T HOFF‖, Martin D. TOBIN¶, Ian P. HALL*, Stuart COOK‡**††, Richard D. GORDON§, Michael STOWASSER§ and Kevin M. O'SHAUGHNESSY‡‡

*Division of Therapeutics and Molecular Medicine, University of Nottingham, Nottingham, U.K.
†NIHR Biomedical Research Unit in Cardiovascular Disease at Royal Brompton and Harefield NHS Foundation Trust and Imperial College London, London, U.K.
‡National Heart and Lung Institute, Imperial College, London, U.K.
§Endocrine Hypertension Research Centre, University of Queensland School of Medicine, Brisbane, Australia
¶Genetic Epidemiology Group, University of Leicester, Leicester, U.K.
‖Paediatric Nephrology Department, Great Ormond Street Hospital for Children, London, U.K.
**Cardiovascular and Metabolic Disorders Program, Duke-National University of Singapore, Singapore
††National Heart Centre Singapore, Singapore
‡‡Clinical Pharmacology Unit, University of Cambridge, Cambridge, U.K.

Abstract

The study of families with rare inherited forms of hypo- and hyper-tension has been one of the most successful strategies to probe the molecular pathophysiology of blood pressure control and has revealed dysregulation of distal nephron Na^+ reabsorption to be a common mechanism. FHHt (familial hyperkalaemic hypertension; also known as Gordon's syndrome) is a salt-dependent form of hypertension caused by mutations in the regulators of the thiazide-sensitive Na^+–Cl^- co-transporter NCC [also known as SLC12A3 (solute carrier family 12 member 3)] and is effectively treated by thiazide diuretics and/or dietary salt restriction. Variation in at least four genes can cause FHHt, including *WNK1* [With No lysine (=K) 1] and *WNK4*, *KLHL3* (kelch-like family member 3), and *CUL3* (cullin 3). In the present study we have identified novel disease-causing variants in *CUL3* and *KLHL3* segregating in 63% of the pedigrees with previously unexplained FHHt, confirming the importance of these recently described FHHt genes. We have demonstrated conclusively, in two unrelated affected individuals, that rare intronic variants in *CUL3* cause the skipping of exon 9 as has been proposed previously. *KLHL3* variants all occur in kelch-repeat domains and so probably disrupt WNK complex binding. We have found no evidence of any plausible disease-causing variants within *SLC4A8* (an alternative thiazide-sensitive sodium transporter) in this population. The results of the present study support the existing evidence that the *CUL3* and *KLHL3* gene products are physiologically important regulators of thiazide-sensitive distal nephron NaCl reabsorption, and hence potentially interesting novel anti-hypertensive drug targets. As a third of our non-*WNK* FHHt families do not have plausible *CUL3* or *KLHL3* variants, there are probably additional, as yet undiscovered, regulators of the thiazide-sensitive pathways.

Key words: diuretic, Gordon's syndrome, hypertension, hyperkalaemia, pseudohypoaldosteronism, thiazide

INTRODUCTION

Hypertension is estimated to contribute 3.5-fold more to the total global disease burden of cardiovascular disease than smoking and 1.6-fold that of hypercholesterolaemia. Worldwide, 20% of deaths in men, 24% of deaths in women, 62% of strokes and 49% of heart disease are attributable to blood pressure [1–3]. The current limitations in anti-hypertensive therapeutics are perhaps not surprising since for most affected individuals the molecular mechanisms driving their hypertension remain undefined.

Although rare, Mendelian forms of hypo- and hyper-tension represent experiments of Nature that have informed our

Abbreviations: CUL3, cullin 3; FHHt, familial hyperkalaemic hypertension; GAN, gigaxonin; IBD, identity by descent; KLHL3, kelch-like family member 3; NCC, Na^+–Cl^- co-transporter; NGS, next-generation sequencing; SLC, solute carrier; SNP, single nucleotide polymorphism; SPAK, STE20/SPS1-related proline/alanine-rich kinase; STE20, sterile 20; WNK, With No lysine (=K).

Correspondence: Dr Mark Glover (email mark.glover@nottingham.ac.uk).

understanding of the physiology of the distal nephron. Remarkably, given the variety of physiological systems that affect arterial pressure, all of these Mendelian syndromes for which the molecular mechanism is understood converge around a common theme: distal nephron sodium wasting in hypotensive syndromes and excessive sodium reabsorption in hypertensive conditions [4].

Although the amiloride-sensitive ENaC (epithelial sodium channel) has classically dominated research interests, NaCl reabsorption via the thiazide-sensitive Na^+–Cl^- co-transporter NCC [also known as SLC12A3 (solute carrier family 12 member 3)] is at least as important [5]. Thiazide diuretics are potent antihypertensive agents [6] and mimic the effects of loss-of-function mutations of NCC observed in the hypotensive monogenic syndrome of Gitelman [7]. Moreover, the heritable condition of FHHt (familial hyperkalaemic hypertension) results from increased sodium reabsorption via NCC and is effectively ameliorated by thiazide diuretics and/or dietary sodium restriction [8].

FHHt is a salt-sensitive hypertension characterized by hyperkalaemic acidosis and exquisite sensitivity to low-dose thiazide diuretics [8,9]. As in Liddle's syndrome [10], significant inter- and intra-pedigree phenotypic variation is observed clinically [11]. Causative variants have been identified in *WNK1* [With No lysine (=K) 1] and *WNK4*, *KLHL3* (kelch-like family member 3), and *CUL3* (cullin 3) [12–15], but not within the NCC itself [16]. Variants are inherited in an autosomal dominant or recessive manner depending on the gene involved and can also occur *de novo* [8,14].

The current model for the regulation of NCC is complex and involves a scaffold of at least 12 interacting proteins centred on a WNK signalling cascade, with intermediary STE20 (sterile 20) kinases [SPAK (STE20/SPS1-related proline/alanine-rich kinase) and OSR1 (oxidative stress-responsive kinase-1)] activated by WNKs which in turn activate NCC [17–19]. CUL3 and KLHL3 are both components of the cullin/Ring E3 ligase ubiquitination pathway and at least some variants of *KLHL3* appear to affect NCC via the control of WNK1 ubiquitination [15,20].

We have identified previously three FHHt pedigrees carrying *WNK4* mutations (D564H, E562K and Q565E) [21], but none carrying *WNK1* mutations. To assess whether our remaining pedigrees with FHHt and without *WNK1/4* mutations had either *CUL3* or *KLHL3* mutations, we undertook NGS (next-generation sequencing) of these genes and also screened an alternative thiazide-sensitive sodium transporter (*SLC4A8*) hypothesized to be an additional candidate [14].

MATERIALS AND METHODS

Study population

The present study was carried out in accordance with the Declaration of Helsinki (2013) of the World Medical Association. Study participants with an FHHt phenotype were identified through tertiary specialist hypertension clinics in the U.K. and Australia. Diagnosis of FHHt was confirmed by the authors. All affected patients were Caucasian and shared a phenotype of persistent hyperkalaemia (plasma potassium >5.0 mmol/l in blood collected without stasis) and hypertension (>140/90 mmHg for adults) following exclusion of the relevant co-morbidities and pharmacotherapies. Detailed phenotypes of the affected individuals are given in Supplementary Figure S1 (at http://www.clinsci.org/cs/126/cs1260721add.htm). All non-affected individuals demonstrated plasma potassium <5 mM/l. The disparity in ages prevented comparison of age-related blood pressure between affected and non-affected individuals. DNA was extracted using a standard method from venous blood acquired following informed consent (Princess Alexandra Hospital Human Research Ethics Committee ID EC00 167 in Australia and National Research Ethics Committee reference 12/EM/0317 in the U.K.).

DNA analysis

CUL3, *KLHL3* and *SLC4A8* genes were sequenced in the affected proband of each family using NGS. PCR amplicons covering all coding exons and exon/intron boundaries were prepared from genomic DNA (Fluidigm Access Array™; the amplicons used are listed in Supplementary Table S1 at http://www.clinsci.org/cs/126/cs1260721add.htm) and sequenced on the Illumina HiSeq platform. Reads were aligned to the human reference sequence hg19 using the Burrows–Wheeler Aligner, and the Genome Analysis Toolkit was used for base recalibration, local realignment and variant calling, following published best practice guidelines, and as described previously [22]. Variants were filtered for rarity and protein consequence: variants altering the protein-coding sequence [missense and nonsense SNPs (single nucleotide polymorphisms), insertions or deletions, or intronic variants at the exon/intron boundary] that were absent from public databases [dbSNP, 1000 Genomes and the NHLBI ESP (National Heart, Lung, and Blood Institute Exome Sequencing Project) Exome Variant Server] were considered candidates. All candidates detected by NGS were confirmed in the proband and assessed for segregation in the pedigree using Sanger sequencing. Variants are reported using Human Genome Variation Society standard nomenclature (http://www.hgvs.org/mutnomen/). The reference sequences used for each gene and protein are listed in Supplementary Table S2 (at http://www.clinsci.org/cs/126/cs1260721add.htm).

RNA studies

The functional effects of putative splice variants were confirmed using RNA studies. Peripheral blood mononuclear cell RNA was isolated from 5 ml of whole blood using a PAXgene blood RNA kit (Qiagen) according to the manufacturer's instructions. The RNA was then transcribed using a Promega AMV reverse transcriptase kit (catalogue number A3500) according to manufacturer's instructions using either random primers (RT1) or a *CUL3*-specific primer (5′-TTATGCTACATATGTGTATACTTTGC-3′; RT2). The resulting cDNA was then PCR-amplified using exon-specific primers to amplify exons 8–10 of the *CUL3* transcript (forward, 5′-TCAACCTCAACTCCAGGTCTCC-3′ and reverse, 5′-TGTTGCCTGAATTCATCCATCG-3′). The PCR products were run on a 2 % agarose gel to visualize them, excised, cleaned using a Promega PCR clean-up kit and Sanger-sequenced on a Beckman CEQ 6800 sequencer. The expected PCR product

sizes were 338 bp and 167 bp for the exon 8–10 and del9 transcripts respectively.

Paralogue mapping

For each gene we first identified paralogues using pre-defined Ensembl protein families (http://www.ensembl.org; release 70), and constructed a multiple sequence alignment using M-Coffee [23]. Reported Mendelian disease-causing variants (non-synonymous SNPs causing a single non-terminal amino acid change) in paralogues of the FHHt genes were identified using the Human Gene Mutation Database Professional version (http://www.hgmd.cf.ac.uk; release 2012.3), and mapped to the equivalent residue of the FHHt gene in the multiple sequence alignment.

Exon-directed array and identity by descent analysis

Representative affected individuals in pedigrees 6, 7 and 8 were genotyped using the Illumina Infinium HumanExome BeadChip array. Pair-wise IBD (identity by descent) analysis was undertaken using PLINK version 1.0.7 [24] on the basis of a subset of 27 402 informative autosomal SNPs with a minor allele frequency >5%. A proportion of IBD (PI_HAT) <0.05 was considered to indicate no excess of sharing (i.e. unrelated individuals).

RESULTS

Genetic analysis of 25 affected individuals from 16 families with FHHt who had already been screened and found negative for *WNK1/4* mutations was performed. A total of 95% of the targeted bases were sequenced adequately for variant calling. The sequencing depth and coverage achieved by gene and exon are shown in Supplementary Figure S2 (at http://www.clinsci.org/cs/126/cs1260721add.htm).

Affected individuals ($n = 16$) from ten of these 16 families were found to have *CUL3* or *KLHL3* variants not reported in the general population (Table 1 and Supplementary Figure S3 at http://www.clinsci.org/cs/126/cs1260721add.htm). We found no evidence of rare variants in *SLC4A8* which segregated with disease phenotype.

As shown in Table 1 and Supplementary Figure S2, affected individuals from eight pedigrees carried variants that have been associated previously with FHHt, two in *CUL3* and six in *KLHL3*. Affected individuals from two pedigrees carried variants unreported previously in *CUL3* (c.1207-12T>A and c.1377 + 1G>T). In addition an affected individual from pedigree 5 was homozygous for a previously reported heterozygous *KLHL3* variant (c.1499G>T; p.G500V) [15]. In keeping with previous observations, *CUL3* mutations were intronic and probably affected splicing of exon 9, whereas *KLHL3* mutations were non-synonymous exonic SNPs (Supplementary Figures S4 and S5 at http://www.clinsci.org/cs/126/cs1260721add.htm).

An affected individual from pedigree 1 had an alternative G>T variant at the same position in *CUL3* as one from pedigree 2 (c.1377 + 1G>C; the original proband reported by Gordon et al. [9]). Both had a severe hyperkalaemic phenotype apparent during

Table 1 *CUL3* and *KLHL3* variants segregating with the FHHt phenotype in each pedigree

The zygosity of affected individuals within each pedigree for the causative variant is shown. Conservation describes the KLHL3 amino acid residues conserved across species expressed as the proportion of species sharing the same reference allele in primates (P), mammals (M) and vertebrates (V) (Ensemble KLHL3 paralogues; available at http://www.ensembl.org/Homo_sapiens/Gene/Compara_Ortholog?g=ENSG00000146021;r=5:136953189-137071779). The country of origin of each pedigree is also shown. Variants are described according to Human Genome Variation Society (HGVS) standard nomenclature using the reference sequences listed in Supplementary Table S2 (at http://www.clinsci.org/cs/126/cs1260721add.htm). *Previously undescribed variants; **previously undescribed genotype.

Pedigree	Gene	Genomic DNA position	HGVS coding DNA position	Zygosity	rs_identity	Protein effect	Conservation	Country of origin
1*	*CUL3*	Chr2:225368368	c.1377 + 1G>T	Heterozygous	–	Exon 9/intron 9 splicing	–	U.K.
2	*CUL3*	Chr2:225368368	c.1377 + 1G>C	Heterozygous	rs199469660	Exon 9/intron 9 splicing	–	Australia
3*	*CUL3*	Chr2:225368551	c.1207–12T>A	Heterozygous	–	Exon 9/intron 8 splicing	–	Australia
4	*CUL3*	Chr2:225368540	c.1207–1G>A	Heterozygous	rs199469654	Exon 9/intron 8 splicing	–	U.K.
5**	*KLHL3*	Chr5:136964078	c.1499G>T	Homozygous	–	G500V	P (9/9), M (37/37), V (49/50)	U.K.
6/7/8	*KLHL3*	Chr5:136974701	c.1160T>C	Heterozygous	rs199469630	L387P	P (9/9), M 33/33), V (46/46)	Australia
9	*KLHL3*	Chr5:136975551	c.1019C>T	Heterozygous	rs199469628	A340V	P (9/9), M 30/31), V (43/44)	Australia
10	*KLHL3*	Chr5:136964097	c.1480G>A	Heterozygous	rs199469633	A494T	P (9/9), M 36/36),	U.K.

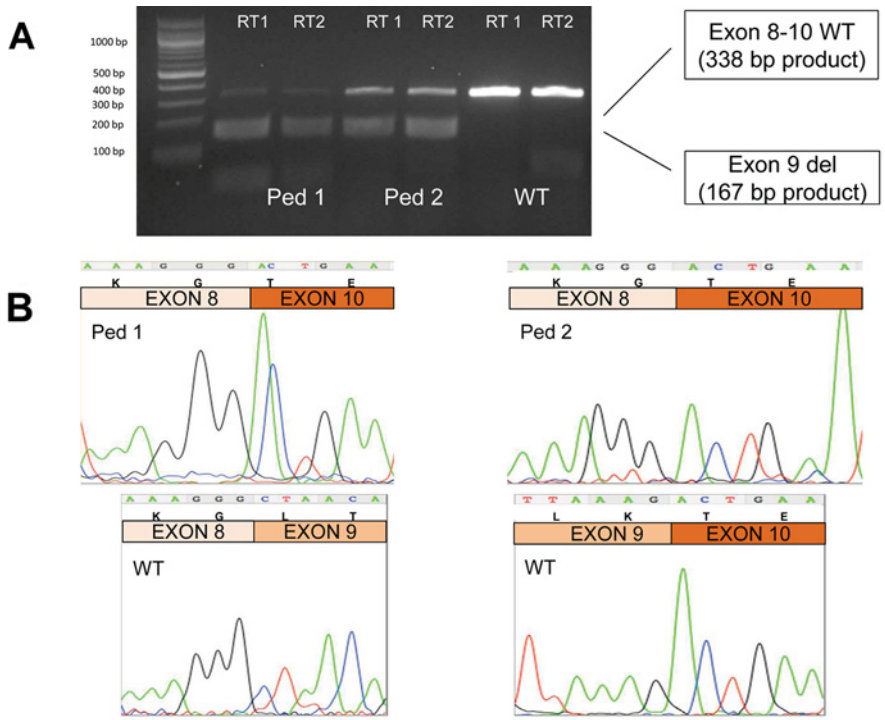

Figure 1 **Demonstration that the *CUL3* variants result in splice variation leading to a loss of exon 9 in affected individuals from pedigree 1 (Ped1) and pedigree 2 (Ped2)**

The affected individuals sequenced are highlighted by * in Supplementary Figure S3 (at http://www.clinsci.org/cs/126/cs1260721add.htm). (**A**) Reverse transcription–PCR of *CUL3* from peripheral blood mononuclear cells demonstrated an additional (smaller) cDNA band only in the affected individuals. The size of the smaller band was consistent with a deficiency of exon 9 (difference in band size = 171 bp). PCR primers RT1 (random primers) and RT2 (a *CUL3*-specific primer) are detailed in the Materials and methods section. The molecular size is given on the left-hand side in bp. (**B**) Sanger sequencing of *CUL3* cDNA from the smaller 167 bp band confirmed that exon 9 is skipped in individuals from both pedigrees. Sequence excerpts from the larger 338 bp band are shown for the wild-type (WT) individual for comparison, demonstrating the wild-type exon boundaries. Sequencing chromatograms are shown together with the DNA sequence and amino acid codons above.

childhood despite coming from different families and living on opposite sides of the globe. Although variants surrounding this exon 9/intron 9 acceptor splice site have been predicted to affect splicing of exon 9 [14], the present study has provided the first evidence of this effect in FHHt patients. Specifically, RNA from peripheral blood monocytes of the index case in pedigrees 1 and 2 contains exon 9-deficient transcripts from the mutated *CUL3* allele (Figure 1).

Pedigrees 6, 7 and 8 all carry the same KLHL3 p.L387P mutation that segregates completely with an FHHt phenotype, raising the question whether these families have a common founder. IBD analysis (Illumina Infinium HumanExome BeadChip) revealed that these pedigrees were no more related than by chance (PI_HAT = 0.0440), indicating that the mutation has probably arisen independently in each lineage. Although the *KLHL3* R528H mutation has also been reported in three pedigrees [15], it was not established whether they shared a common founder. Hence in our pedigrees, KLHL3 p.L378P is the most commonly identified FHHt-causing *KLHL3* mutation with robust evidence of independent founder mutations.

To assess the pathogenicity of the KLHL3 variants associated with FHHt, we used a Paralogue Annotation approach [25]. KLHL3 is one of a family of evolutionarily related cytoskeletal BTB/kelch repeat proteins, variation in several of which cause Mendelian disease. Using multiple sequence alignment to identify structurally and functionally equivalent residues across the protein family, we observed that one of the KLHL3 variants reported previously to be associated with FHHt [14,15] (KLHL3 p.R384W) co-locates with a reported disease-causing variant in another member of the protein family KBTBD13 p.R248S {where KBTBD13 is kelch repeat and BTB [BR-C (Broad Complex), ttk (tramtrack) and bab (bric a brac)] (POZ) domain-containing 13}, which is associated with nemalin myopathy [26]. This suggests that the variants lie at a functionally important site conserved across the protein family that is intolerant of sequence variation. Similarly, two of the KLHL3 FHHt variants in our patients (L387P and A494T) are very close to the location of known disease-causing variants in GAN (gigaxonin) [27], suggesting that these too are probably functionally important sites. GAN p.G368 and p.G474 (at which substitutions are associated with giant axonal neuropathy [27]) are equivalent to KLHL3 p.G388 and p.G496, and are adjacent to rare variants found in our FHHt pedigrees.

DISCUSSION

In the present study we have identified disease-causing variants in *CUL3* and *KLHL3* in 63% of our pedigrees with FHHt who had been screened and found to be negative for *WNK1/4* mutations, confirming recent reports of association between *CUL3* and *KLHL3* variants and FHHt [14,15]. In the case of *CUL3* mutation at position c.1377 + 1 we report a second variant allele associated with a similar thiazide-responsive FHHt phenotype, strengthening further the case for a functional role of aberrant CUL3 function on sodium reabsorption in the distal nephron. We have also demonstrated that the predicted exon 9 splicing effect produced by c.1377 + 1G>T and c.1377 + 1G>A is, in fact, observed.

We have found that KLHL3 p.L387P associated with FHHt in three unrelated pedigrees, making this the most commonly occurring single FHHt mutation not only within our FHHt consortium, which includes three FHHt pedigrees carrying different WNK4 mutations (D564H, E562K and Q565E) [21], but also among all *KLHL3* mutations reported to date [14,15]. That *KLHL3* variants in our pedigrees are restricted to kelch repeats, and that other FHHt-associated *KLHL3* variants cluster in these domains provides further support for disruption of WNK complex binding as reported previously [20].

Accepting the limitations of bioinformatics tools to predict pathogenicity, we did not find evidence of probable disease-causing variants within an alternative thiazide-sensitive sodium bicarbonate exchanger, *SLC4A8*, hypothesized as an alternative genetic candidate for FHHt [14]. A third of our pedigrees with non-*WNK* FHHt therefore remain without a genetic diagnosis, which is somewhat greater than that reported in other pedigree collections [14,15]. This highlights the genetic heterogeneity of the FHHt phenotype and the likelihood that additional, as yet undiscovered, regulators of thiazide-sensitive pathways exist. It is also worth emphasizing that we set out to identify *KLHL3* and *CUL3* variants in subjects with a clinical diagnosis of FHHt on the basis of measurements routinely recorded in the clinic. Similar data are recorded for unaffected relatives, but because of the large disparity in ages it is often impossible to provide a comparison of age-related blood pressure between affected and non-affected individuals. Nevertheless, all non-affected individuals were normokalaemic with a plasma potassium <5 mmol/l, and we are confident that we have correctly assigned affected compared with non-affected status within our pedigrees.

Further detailed laboratory and clinical studies are required to establish whether the effects of the reported heterogeneity of variant *KLHL3* on WNK1 immunoprecipitation and ubiquitination translate into differential effects on thiazide-sensitive distal nephron sodium trafficking and phenotype within FHHt [20]. For instance, do patients with KLHL3 A340V and A494T Gordon's syndrome have the same CUL3/KLHL3/WNK/SPAK/NCC pathway abnormalities as those with KLHL3 L387P?

In conclusion we have identified disease-causing variants in *CUL3* and *KLHL3* in patients with FHHt screened previously and found to be negative for *WNK1* and *WNK4* mutations, but did not find evidence of such variants in the alternative candidate *SLC4A8*. Approximately one-third of our non-WNK patients with FHHt remain without a molecular diagnosis raising the possibility that there may be additional regulators of thiazide-sensitive distal nephron sodium trafficking which remain to be discovered.

CLINICAL PERSPECTIVES

- The present study was performed to acertain whether pedigress with FHHt, but without mutation in *WNK1/WNK4*, contained mutation in *CUL3*, *KLHL3* or *SLC4A8*.
- The present study confirms recent findings of *CUL3* and *KLHL3* mutations in FHHt and identifies novel disease-causing variants. This strengthens the argument that these gene products are physiologically important regulators of distal nephron NaCl reabsorption via thiazide-sensitive pathways, and hence are potentially interesting novel anti-hypertensive drug targets.
- As only 63% of our non-*WNK* FHHt families were found to contain plausible *CUL3* or *KLHL3* variants, there are probably additional, as yet undiscovered, regulators of thiazide-sensitive pathways.

AUTHOR CONTRIBUTION

Mark Glover, James Ware, Ian Hall, Richard Gordon, Michael Stowasser and Kevin O'Shaughnessy designed the study and drafted the paper. Mark Glover, Martin Wolley, Shengxin Xu, William Van't Hoff, Richard Gordon, Michael Stowasser and Kevin O'Shaughnessy collected the patient material. Mark Glover, James Ware, Kevin O'Shaughnessy and Amanda Henry performed and analysed *CUL3*, *KLHL3* and *SLC4A8* genetic sequencing. Louise Wain and Martin Tobin undertook the IBD analysis. Roddy Walsh, James Ware and Stuart Cook performed the paralogue mapping.

FUNDING

This work was supported by the Academy of Medical Sciences via a grant for Clinical Lecturers (to M.G. and J.S.W.), the British Heart Foundation [grant number PG/09/089 (to K.M.O.)], an Irene Patricia Hunt Memorial Bequest to the University of Queensland for Research into Hypertension (to M.W, R.D.G. and M.S.), the National Health and Medical Research Council of Australia (to S.X.), the National Institute for Health Research Royal Brompton Cardiovascular Biomedical Research Unit (to J.S.W., R.W. and S.C.), Fondation Leducq (to J.S.W., R.W., and S.C.) and the British Heart Foundation (J.S.W., R.W. and S.C.) and the Medical Research Council via a Senior Clinical Fellowship [grant number G0902313 (to M.D.T.)].

REFERENCES

1 World Health Organization (2002) The World Health Report 2002: Reducing Risks, Promoting Healthy Life, World Health Organization, Geneva (http://www.who.int/whr/2002/en/)
2 World Health Organization (2010) Global Status Report on Noncommunicable Diseases 2010, World Health Oraganization, Geneva (http://www.who.int/nmh/publications/ncd_report_full_en.pdf)

3 Cardiovascular Health Working Group of the Faculty of Public Health (2005) Easing the Pressure: Tackling Hypertension, Faculty of Public Health and the National Heart Forum, London (http://www.fph.org.uk/uploads/hypertendion_all.pdf)
4 Lifton, R. P., Gharavi, A. G. and Geller, D. S. (2001) Molecular mechanisms of human hypertension. Cell **104**, 545–556
5 Glover, M., Mercier Zuber, A. and O'Shaughnessy, K. M. (2011) Hypertension, dietary salt intake, and the role of the thiazide-sensitive sodium chloride transporter NCCT. Cardiovasc. Ther. **29**, 68–76
6 National Institute for Health and Clinical Excellence, (2011) Hypertension: Clinical Management of Primary Hypertension in Adults. Clinical Guideline CG127, National Institute for Health and Clinical Excellence, London (http://guidance.nice.org.uk/CG127)
7 Simon, D. B., Nelson-Williams, C., Bia, M. J., Ellison, D. H., Karet, F. E., Molina, A. M., Vaara, I., Iwata, F., Cushner, H. M., Koolen, M. and Lifton, R. P. (1996) Gitelman's variant of Bartter's syndrome, inherited hypokalaemic alkalosis, is caused by mutations in the thiazide-sensitive NaCl transporter. Nat. Genet. **12**, 24–30
8 Gordon, R. D. (1986) The syndrome of hypertension and hyperkalemia with normal glomerular filtration rate: Gordon's syndrome. Aust. N. Z. J. Med. **16**, 183–184
9 Gordon, R. D., Geddes, R. A., Pawsey, C. G. K. and O'Halloran, M. W. (1970) Hypertension and severe hyperkalaemia associated with suppression of renin and aldosterone and completely reversed by dietary sodium restriction. Aust. Ann. Med. **19**, 287–294
10 Jeunemaitre, X., Bassilana, F., Persu, A., Dumont, C., Champigny, G., Lazdunski, M., Corvol, P. and Barbry, P. (1997) Genotype-phenotype analysis of a newly discovered family with Liddle's syndrome. J. Hypertens. **15**, 1091–1100
11 Gordon, R. D. (1986) Syndrome of hypertension and hyperkalemia with normal glomerular filtration rate. Hypertension **8**, 93–102
12 Disse-Nicodeme, S., Achard, J. M., Desitter, I., Hout, A., Fournier, A., Corvol, P. and Jeunemaitre, X. (2000) A new locus on chromosome 12p 13.3 for pseudohypoaldosteronism type II, an autosomal dominant form of hypertension. Am. J. Hum. Genet. **67**, 302–310
13 Mansfield, T. A., Simon, D. B., Farfel, Z., Bia, M., Tucci, J. R., Lebel, M., Gutkin, M., Vialettes, B., Christofilis, M. A., Kauppinen-Makelin, R. et al. (1997) Multilocus linkage of familial hyperkalaemia and hypertension, pseudohypoaldosteronism type II, to chromosomes 1q31-42 and 17p11-q21. Nat. Genet. **16**, 202–205
14 Boyden, L. M., Choi, M., Choate, K. A., Nelson-Williams, C. J., Farhi, A., Toka, H. R., Tikhonova, I. R., Bjornson, R., Mane, S. M., Colussi, G. et al. (2012) Mutations in kelch-like 3 and cullin 3 cause hypertension and electrolyte abnormalities. Nature **482**, 98–102
15 Louis-Dit-Picard, H., Barc, J., Trujillano, D., Miserey-Lenkei, S., Bouatia-Naji, N., Pylypenko, O., Beaurain, G., Bonnefond, A., Sand, O., Simian, C. et al. (2012) KLHL3 mutations cause familial hyperkalemic hypertension by impairing ion transport in the distal nephron. Nat. Genet. **44**, 456–460
16 Disse-Nicodeme, S., Desitter, I., Fiquet-Kempf, B., Hout, A., Stern, N., Delagousse, M., Potier, J., Ader, J. and Jeunemaitre, X. (2001) Genetic heterogeneity of familial hyperkalaemic hypertension. J. Hypertens. **19**, 1957–1964
17 Glover, M., Mercier Zuber, A. and O'Shaughnessy, K. M. (2009) Renal and brain isoforms of WNK3 have opposite effects on NCCT. J. Am. Soc. Nephrol. **20**, 1314–1322
18 Glover, M., Mercier Zuber, A., Figg, N. and O'Shaughnessy, K. M. (2010) The activity of the thiazide-sensitive Na^+–Cl^- cotransporter is regulated by protein phosphatase, PP4. Can. J. Physiol. Pharmacol. **88**, 986–995
19 Rafiqi, F. H., Mercier Zuber, A., Glover, M., Richardson, C., Fleming, S., Jovanovic, S., Jovanovic, A., O'Shaughnessy, K. M. and Alessi, D. R. (2010) Role of the WNK-activated SPAK kinase in regulating blood pressure. EMBO Mol. Med. **2**, 1–13
20 Ohta, A., Schumacher, F-R., Mehellou, Y., Johnson, C., Knebel, A., Macartney, T. J., Wood, N. T., Alessi, D. R. and Kurz, T. (2013) The CUL3–KLHL3 E3 ligase complex mutated in Gordon's hypertension syndrome interacts with and ubiquitylates WNK isoforms; disease-causing mutations in KLHL3 and WNK4 disrupt interaction. Biochem. J. **45**, 111–122
21 Golbang, A. P., Murthy, M., Hamad, A., Liu, C-H., Cope, G., Van't Hoff, W., Cuthbert, A. W. and O'Shaughnessy, K. M. (2005) A new kindred with pseudohypoaldosteronism type II and a novel mutation (564D>H) in the acidic motif of the *WNK4* gene. Hypertension **46**, 295–300
22 Li, X., Buckton, A. J., Wilkinson, S. L., John, S., Walsh, R., Novotny, T., Valaskova, I., Gupta, M., Game, L., Barton, P. J. R. et al. (2013) Towards clinical molecular diagnosis of inherited cardiac conditions: a comparison of bench-top genome DNA sequencers. PLoS ONE **8**, e67744
23 Moretti, S., Armougom, F., Wallace, I. M., Higgins, D. G., Jongeneel, C. V. and Notredame, C. (2007) The M-Coffee web server: a meta-method for computing multiple sequence alignments by combining alternative alignment methods. Nucleic Acids Res. **35**, W645–W648
24 Purcell, S., Neale, B., Todd-Brown, K., Thomas, L., Ferreira, M. A., Bender, D., Maller, J., Sklar, P., de Bakker, P. I., Daly, M. J. and Sham, P. C. (2007) PLINK: a tool set for whole-genome association and population-based linkage analyses. Am. J. Hum. Genet. **81**, 559–575
25 Ware, J. S., Walsh, R., Cunningham, F., Birney, E. and Cook, S. (2012) Paralogous annotation of disease-causing variants in long QT syndrome genes. Hum. Mutat. **33**, 1188–1191
26 Sambuughin, N., Yau, K. S., Olivé, M., Duff, R. M., Bayarsaikhan, M., Lu, S., Gonzalez-Mera, L., Sivadorai, P., Nowak, K. J., Ravenscroft, G. et al. (2010) Dominant mutations in KBTBD13, a member of the BTB/Kelch family, cause nemaline myopathy with cores. Am. J. Hum. Genet. **87**, 842–847
27 Bomont, P., Cavalier, L., Blondeau, F., Hamida, C. B., Belal, S., Tazir, M., Demir, E., Topaloglu, H., Korinthenberg, R., Tuysuz, B. et al. (2000) The gene encoding gigaxonin, a new member of the cytoskeletal BTB/kelch repeat family, is mutated in giant axonal neuropathy. Nat. Genet. **26**, 370–374

Received 28 June 2013/11 November 2013; accepted 25 November 2013
Published as Immediate Publication 25 November 2013, doi: 10.1042/CS20130326

Clinical Science (2014) **126**, 721–726 (Printed in Great Britain) doi: 10.1042/CS20130326

online data

Original Paper

SUPPLEMENTARY ONLINE DATA

Detection of mutations in *KLHL3* and *CUL3* in families with FHHt (familial hyperkalaemic hypertension or Gordon's syndrome)

Mark GLOVER*, James S. WARE†‡, Amanda HENRY*, Martin WOLLEY§, Roddy WALSH†, Louise V. WAIN¶, Shengxin XU§, William G. VAN'T HOFF‖, Martin D. TOBIN¶, Ian P. HALL*, Stuart COOK‡**††, Richard D. GORDON§, Michael STOWASSER§ and Kevin M. O'SHAUGHNESSY‡‡

*Division of Therapeutics and Molecular Medicine, University of Nottingham, Nottingham, U.K.
†NIHR Biomedical Research Unit in Cardiovascular Disease at Royal Brompton and Harefield NHS Foundation Trust and Imperial College London, London, U.K.
‡National Heart and Lung Institute, Imperial College, London, U.K.
§Endocrine Hypertension Research Centre, University of Queensland School of Medicine, Brisbane, Australia
¶Genetic Epidemiology Group, University of Leicester, Leicester, U.K.
‖Paediatric Nephrology Department, Great Ormond Street Hospital for Children, London, U.K.
**Cardiovascular and Metabolic Disorders Program, Duke-National University of Singapore, Singapore
††National Heart Centre Singapore, Singapore
‡‡Clinical Pharmacology Unit, University of Cambridge, Cambridge, U.K.

Supplementary Figures S1–S5 and Tables S1 and S2 can be found on the following pages.

Correspondence: Dr Mark Glover (email mark.glover@nottingham.ac.uk).

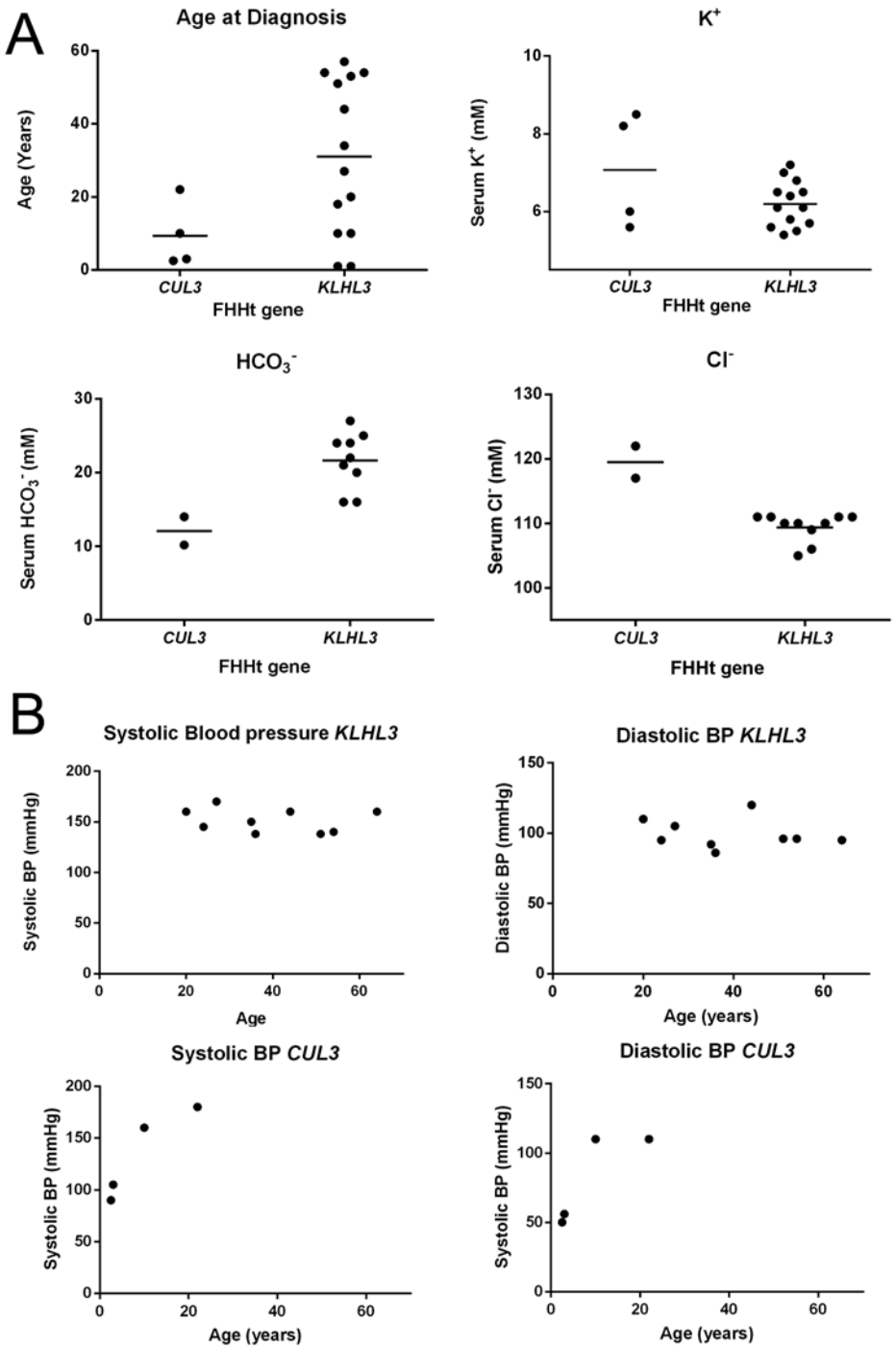

Figure S1 Clinical features in FHHt-affected individuals stratified by genotype

(**A**) Age at diagnosis and serum K^+, HCO_3^- and Cl^- are shown for FHHt-affected individuals with mutations in *CUL3* and *KLHL3*. (**B**) Systolic and diastolic blood pressure (BP) for FHHt-affected individuals of each mutation class is shown as a function of age.

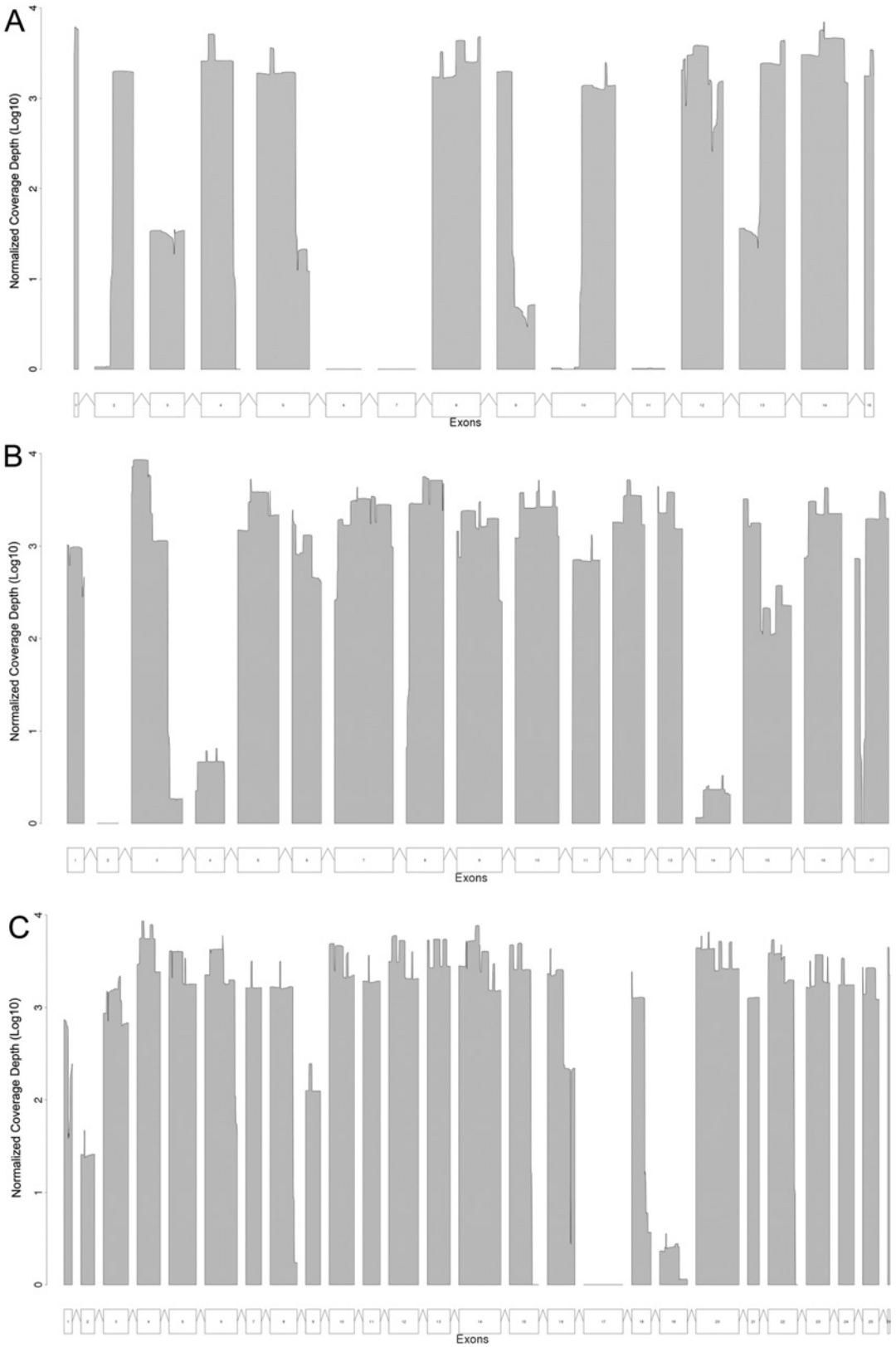

Figure S2 **Average depth of sequencing for (A) *KLHL3*, (B) *CUL3* and (C) *SLC4A8* genes enriched using the Fluidigm Access Array™ by exon**
Log_{10} normalized depth of coverage is shown against DNA position with numbered exons in each case.

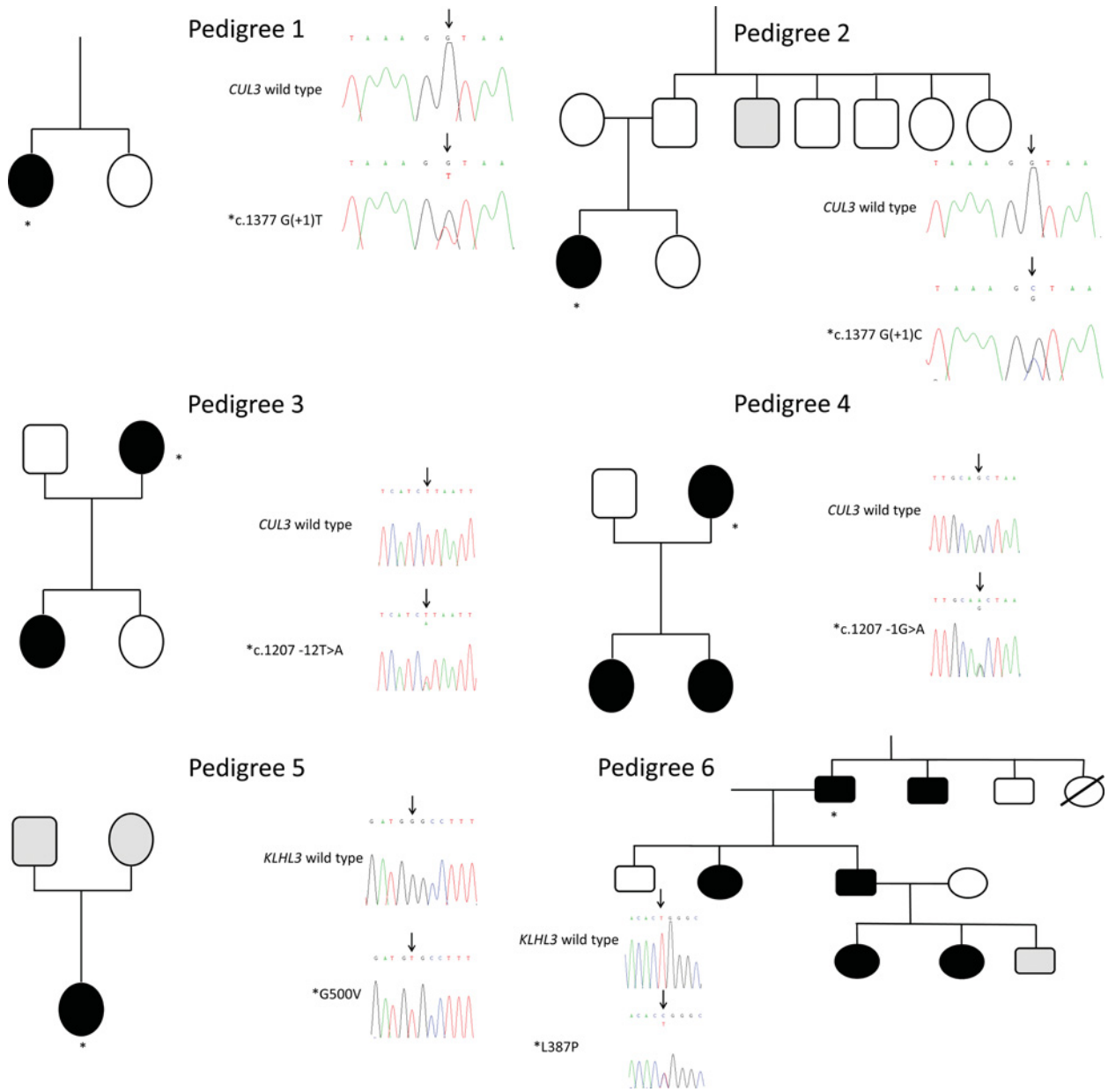

Figure S3 **Pedigree structure of the ten kindreds with FHHt and mutations in *CUL3* and *KLHL3* detailed in Table 1 of the main text**

Affected, unaffected and phenotype-undetermined subjects are denoted by black, white and grey symbols respectively. Alongside each pedigree, Sanger sequence traces are shown showing the wild-type sequence and the corresponding *CUL3* or *KLHL3* variant segregating with the affected phenotype within each family. *The affected individual whose sequence is shown; c, the following co-ordinate is of coding DNA. Variants are described using standard Human Genome Variation Society nomenclature. Reference sequences for each gene are listed in Table S1. Pedigree 1: the affected individual carries a previously unreported variant disrupting a consensus splice site in *CUL3*. The lower chromatogram of *CUL3* shows that in the affected individual the wild-type guanine at position c.1377 + 1 (the first base of intron 9 at the border with exon 9) is mutated to thymine in a heterozygous manner compared with the wild-type chromatogram shown above. The position of this variant is shown in more detail in Figure S5 and full genetic co-ordinates are detailed in Table 1 of the main text. Pedigree 2: the affected individual carries a previously reported variant co-locating with the variant observed in pedigree 1, which also disrupts the consensus splice site in *CUL3*. The lower chromatogram shows that in the affected individual the wild-type guanine at position c.1377 + 1 (the first base of intron 9 on the border with exon 9) is mutated to cytosine in a heterozygous manner compared with the wild-type chromatogram above. The position of this variant is shown in more detail in Figure S5 and full genetic co-ordinates are detailed in Table 1 of the main text. Pedigree 3: the affected individual carries a previously unreported splice region variant close to a consensus splice site at the border of exon 9 in *CUL3*. The lower chromatogram of *CUL3* shows that in the affected individual the wild-type thymine,12 bases into intron 8 from the exon 9 border position c.1207, is mutated to adenine in a heterozygous manner compared with the wild-type

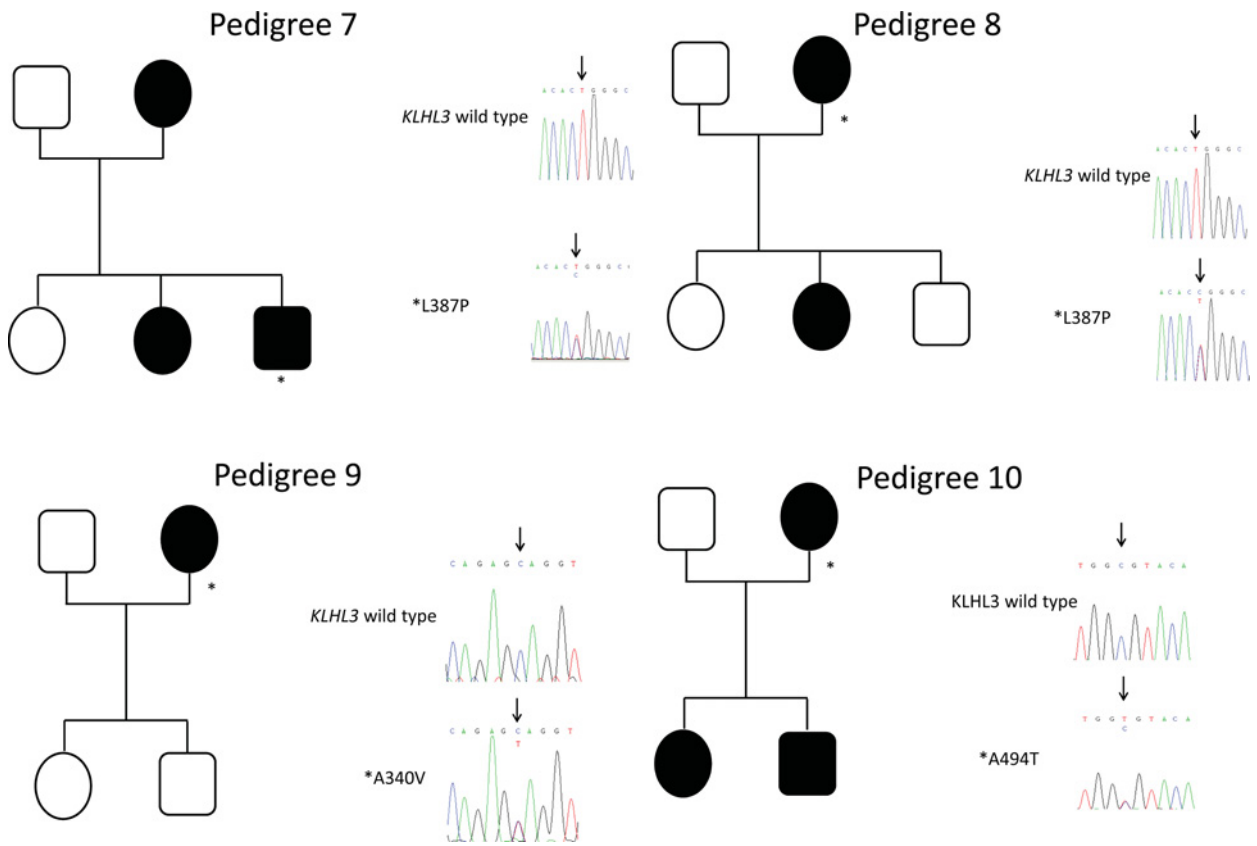

Figure S3 Continued

chromatogram above. The position of this variant is shown in more detail in Figure S5 and full genetic co-ordinates are detailed in Table 1 of the main text. Pedigree 4: the affected individual carries a previously reported variant disrupting a consensus splice site at the border of exon 9 in *CUL3*. The lower chromatogram of *CUL3* shows that in the affected individual the wild-type guanine, one base into intron 8 from the exon 9 border position c.1207, is mutated to adenine in a heterozygous manner compared with the wild-type chromatogram above. The position of this variant is shown in more detail in Figure S5 and full genetic co-ordinates are detailed in Table 1 of the main text. Pedigree 5: the affected individual carries a previously reported FHHt-associated missense variant in *KLHL3*. The lower chromatogram of *KLHL3* shows that in the affected individual the wild-type guanine is mutated to thymine in a homozygous manner compared with the wild-type chromatogram. This leads to exon 13 of *KLHL3* encoding the amino acid mutation G500V. The position of this mutation is shown in more detail in Figure S4 and full genetic co-ordinates are detailed in Table 1 of the main text. Pedigree 6: the affected individual carries a previously reported FHHt-associated missense variant in *KLHL3*. The lower chromatogram of *KLHL3* shows that in the affected individual the wild-type thymine is mutated to cytosine in a heterozygous manner compared with the wild-type chromatogram. This leads to exon 10 of *KLHL3* encoding the amino acid change L387P. The position of this mutation is shown in more detail in Figure S4 and full genetic co-ordinates are detailed in Table 1 of the main text. Pedigree 7: the affected individual carries a previously reported FHHt-associated missense variant in *KLHL3*. The lower chromatogram of *KLHL3* shows that in the affected individual the wild-type thymine is mutated to cytosine in a heterozygous manner compared with the wild-type chromatogram. This leads to exon 10 of *KLHL3* encoding the amino acid mutation L387P. The position of this mutation is shown in more detail in Figure S4 and full genetic co-ordinates are detailed in Table 1 of the main text. Pedigree 8: the affected individual carries a previously reported FHHt-associated missense variant in *KLHL3*. The lower chromatogram of *KLHL3* shows that in the affected individual the wild-type thymine is mutated to cytosine in a heterozygous manner compared with the wild-type chromatogram. This leads to exon 10 of *KLHL3* encoding the amino acid mutation L387P. The position of this mutation is shown in more detail in Figure S4 and full genetic co-ordinates are detailed in Table 1 of the main text. Pedigree 9: the affected individual carries a previously reported FHHt-associated missense variant in *KLHL3*. The lower chromatogram of *KLHL3* shows that in the affected individual the wild-type cytosine is mutated to thymine in a heterozygous manner compared with the wild-type chromatogram. This leads to exon 9 of *KLHL3* encoding the amino acid mutation A340V. The position of this mutation is shown in more detail in Figure S4 and full genetic co-ordinates are detailed in Table 1 of the main text. Pedigree 10: the affected individual carries a previously reported FHHt-associated missense variant in *KLHL3*. The lower chromatogram of *KLHL3* shows that in the affected individual the wild-type cytosine is mutated to thymine in a heterozygous manner compared with the wild-type chromatogram. This leads to exon 13 of *KLHL3* encoding the amino acid mutation A494T. The position of this mutation is shown in more detail in Figure S4 and full genetic co-ordinates are detailed in Table 1 of the main text.

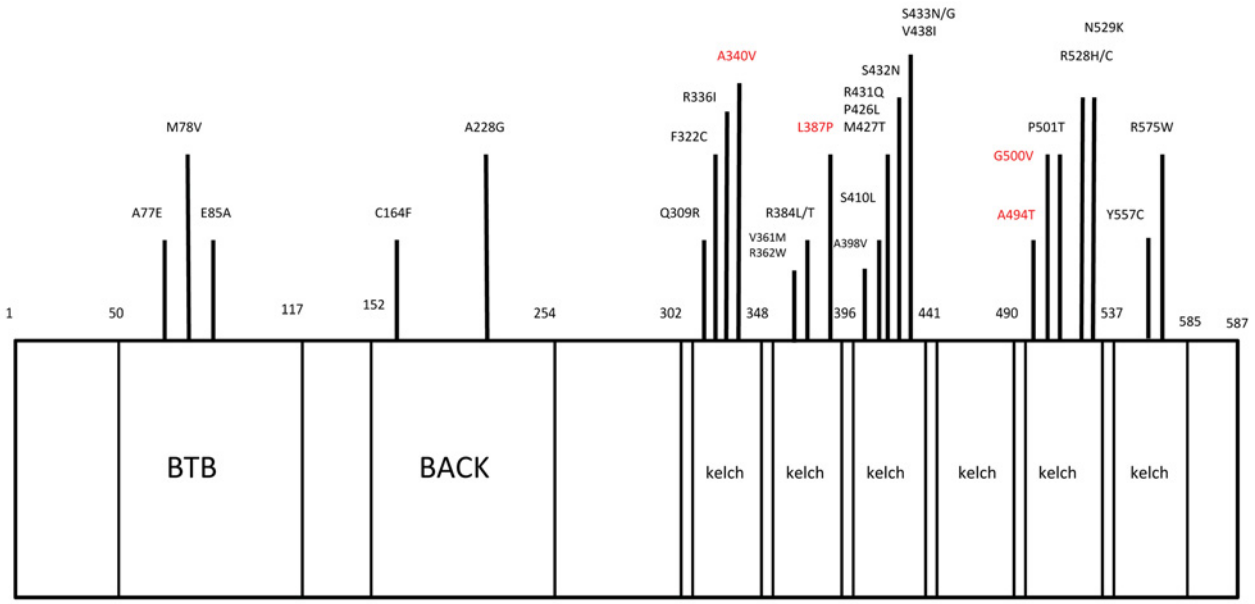

Figure S4 **A schematic diagram illustrating the location of FHHt-associated variants in the KLHL3 protein**
Variants identified in the present study are highlighted in red. KLHL3 variants cluster in the kelch domains. The domain structure of KLHL3 includes BTB [BR-C (Broad Complex), ttk (tramtrack) and bab (bric a brac)], BACK and C-terminal kelch domains.

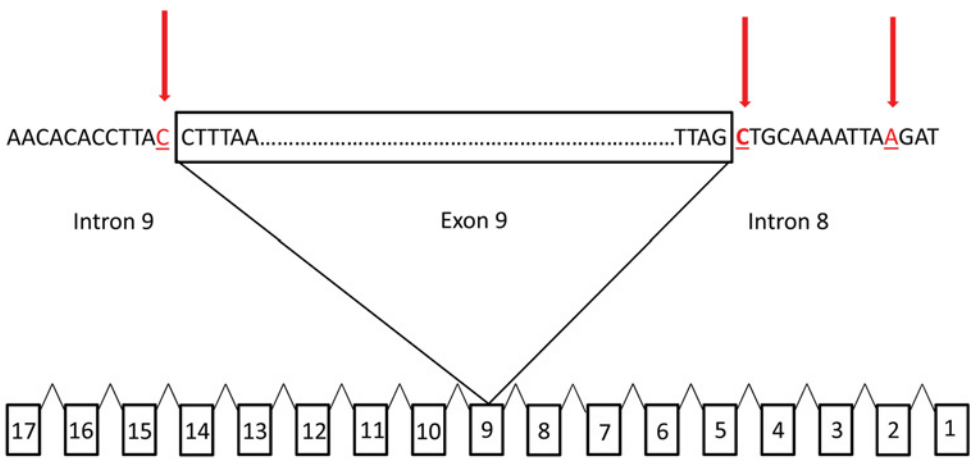

Figure S5 ***CUL3* variants found in affected individuals with FHHt cluster at exon 9 splice sites and cause skipping of this exon**
The 17 exons of *CUL3* are depicted and the *CUL3* variants associated with FHHt clustering at either end of the exon 9 borders are shown. Positions found mutated in the present study are coloured red.

Table S1 Genomic DNA targets amplified by the Fluidigm Access Array™ for the *CUL3*, *KLHL3* and *SLC4A8* genes

Gene	Amplicon number	Location
KLHL3	KLHL3_t1	Chr5:136961441–136961585
KLHL3	KLHL3_t2	Chr5:136957785–136957815
KLHL3	KLHL3_t3	Chr5:136963985–136964126
KLHL3	KLHL3_t4	Chr5:136969725–136969854
KLHL3	KLHL3_t5	Chr5:136972982–136973084
KLHL3	KLHL3_t6	Chr5:136974641–136974839
KLHL3	KLHL3_t7	Chr5:136975548–136975666
KLHL3	KLHL3_t8	Chr5:136993819–136993969
KLHL3	KLHL3_t9	Chr5:136997603–136997720
KLHL3	KLHL3_t10	Chr5:137013233–137013343
KLHL3	KLHL3_t11	Chr5:137027973–137028136
KLHL3	KLHL3_t12	Chr5:137033975–137034097
KLHL3	KLHL3_t13	Chr5:137045438–137045545
KLHL3	KLHL3_t14	Chr5:137056153–137056273
KLHL3	KLHL3_t15	Chr5:137071321–137071336
CUL3	CUL3_t1	Chr2:225449660–225449727
CUL3	CUL3_t2	Chr2:225422375–225422573
CUL3	CUL3_t3	Chr2:225400244–225400358
CUL3	CUL3_t4	Chr2:225379328–225379489
CUL3	CUL3_t5	Chr2:225378240–225378355
CUL3	CUL3_t6	Chr2:225376070–225376299
CUL3	CUL3_t7	Chr2:225371574–225371720
CUL3	CUL3_t8	Chr2:225370672–225370849
CUL3	CUL3_t9	Chr2:225368368–225368539
CUL3	CUL3_t10	Chr2:225367681–225367789
CUL3	CUL3_t11	Chr2:225365079–225365204
SLC4A8	SLC4A8_t21	Chr12:51888728–51888902
SLC4A8	SLC4A8_t22	Chr12:51890770–51890963
SLC4A8	SLC4A8_t23	Chr12:51897812–51897904
SLC4A8	SLC4A8_t24	Chr12:51899618–51899714
SLC4A8	SLC4A8_t25	Chr12:51901209–51901223
CUL3	CUL3_t12	Chr2:225362469–225362566
CUL3	CUL3_t13	Chr2:225360548–225360683
SLC4A8	SLC4A8_t1	Chr12:51818770–51818819
SLC4A8	SLC4A8_t2	Chr12:51834491–51834573
SLC4A8	SLC4A8_t3	Chr12:51844659–51844806
SLC4A8	SLC4A8_t4	Chr12:51845907–51846043
SLC4A8	SLC4A8_t5	Chr12:51847322–51847483
SLC4A8	SLC4A8_t6	Chr12:51851134–51851323
SLC4A8	SLC4A8_t7	Chr12:51852342–51852434
SLC4A8	SLC4A8_t8	Chr12:51853734–51853892
SLC4A8	SLC4A8_t9	Chr12:51854987–51855075
SLC4A8	SLC4A8_t10	Chr12:51856093–51856240
SLC4A8	SLC4A8_t11	Chr12:51857397–51857498
SLC4A8	SLC4A8_t12	Chr12:51863397–51863572
SLC4A8	SLC4A8_t13	Chr12:51864175–51864309
SLC4A8	SLC4A8_t14	Chr12:51865070–51865316
SLC4A8	SLC4A8_t15	Chr12:51868125–51868231
SLC4A8	SLC4A8_t16	Chr12:51868828–51868990
SLC4A8	SLC4A8_t17	Chr12:51879570–51879684
SLC4A8	SLC4A8_t18	Chr12:51882482–51882644
SLC4A8	SLC4A8_t19	Chr12:51883483–51883735
SLC4A8	SLC4A8_t20	chr12:51887487–51887556

Table S2 Transcript and protein identities used for the variant descriptions in the present study

GAN, gigatoxin; KBTBD13, kelch repeat and BTB (POZ) domain-containing 13; KLHL, kelch-like.

Gene	Ensembl transcript	Ensembl protein
WNK1	ENST00000315939	ENSP00000313059
WNK4	ENST00000246914	ENSP00000246914
CUL3	ENST00000264414	ENSP00000264414
KLHL3	ENST00000309755	ENSP00000312397
SLC4A8	ENST00000453097	ENSP00000405812
GAN	ENST00000248272	ENSP00000248272
SLC4A1	ENST00000262418	ENSP00000262418
KLHL10	ENST00000293303	ENSP00000293303
KLHL7	ENST00000339077	ENSP00000343273
SLC4A4	ENST00000340595	ENSP00000344272
KLHL9	ENST00000359039	ENSP00000351933
SLC4A11	ENST00000380056	ENSP00000369396
CUL5	ENST00000393094	ENSP00000376808
CUL4B	ENST00000404115	ENSP00000384109
KBTBD13	ENST00000432196	ENSP00000388723

Received 28 June 2013/11 November 2013; accepted 25 November 2013

Published as Immediate Publication 25 November 2013, doi: 10.1042/CS20130326